Journal of Maps

ISSN: (Print) (Online) Journal homepage: www.tandfonline.com/journals/tjom20

Geology of the polyphase Olympica – Jovis Fossae channel system

Anita Zambrowska, Daniel Mège & Sam Poppe

To cite this article: Anita Zambrowska, Daniel Mège & Sam Poppe (2024) Geology of the polyphase Olympica – Jovis Fossae channel system, Journal of Maps, 20:1, 2419467, DOI: 10.1080/17445647.2024.2419467

To link to this article: https://doi.org/10.1080/17445647.2024.2419467

© 2024 The Author(s). Published by Informa UK Limited, trading as Taylor & Francis Group on behalf of Journal of Maps

View supplementary material

Published online: 30 Oct 2024.

Submit your article to this journal

View related articles

View Crossmark data

Full Terms & Conditions of access and use can be found at
https://www.tandfonline.com/action/journalInformation?journalCode=tjom20

JOURNAL OF MAPS
2024, VOL. 20, NO. 1, 2419467
https://doi.org/10.1080/17445647.2024.2419467

Taylor & Francis
Taylor & Francis Group

Science

OPEN ACCESS Check for updates

Geology of the polyphase Olympica – Jovis Fossae channel system

Anita Zambrowska, Daniel Mège and Sam Poppe

Centrum Badań Kosmicznych Polskiej Akademii Nauk (CBK PAN), Warszawa, Poland

ABSTRACT

Outflow channels of the Tharsis province on Mars testify to the drainage of groundwater reservoirs through magmatic and tectonic processes. The Olympica – Jovis Fossae system extends over 500 km, but the significance of its deep and narrow channels for the Tharsis dome is poorly understood. We present a new geologic map of Olympica-Jovis Fossae where we mapped landforms and geological units, dated them relatively, and identified the chronological succession of outflow events and deposition of lava flows, airfall, and sedimentary units. Cross-cutting relationships indicate a complex succession of 28 channel incisions in the volcanic stratigraphy. The five identified morphological channel types indicate different flow dynamics at different times and places. The map highlights the role of intensive volcanic activity in releasing water from overpressurized aquifers and possible subglacial flows, and will assist in a better understanding of the general conditions for catastrophic groundwater flooding in a volcanic context.

Key policy highlights

- We present a detailed geologic map of Olympica and Jovis Fossae in the Tharsis volcanic province on Mars.
- We identified 28 channels classified into five morphological types.
- Cross-cutting channel relationships demonstrate a polyphase development of the system.

ARTICLE HISTORY
Received 3 July 2024
Revised 14 October 2024
Accepted 15 October 2024

KEYWORDS
Mars; outburst flood; outflow channel; lava flow; glacial channel; fluvial channel

1. Introduction

Mars, like Earth, bears the scars of a dynamic past, shaped by various geological processes such as tectonic, hydrologic, and volcanic activity. The Tharsis region is the broadest and most complex of the volcanic provinces on Mars and boasts several major volcanoes: Olympus Mons, Alba Mons, and Tharsis Montes: Arsia Mons, Pavonis Mons, and Ascraeus Mons (Cassanelli & Head, 2019; Werner, 2009). The formation of the largest volcano, Olympus Mons, started in the Hesperian (Werner, 2009). The first deformations of the growing Tharsis date to 3.7 billion years ago (Bouley et al., 2016; Carr & Head, 2010), while the youngest lava flows date back to the Late Amazonian epoch (Neukum et al., 2004).

The first map of the Tharsis region based on Viking pictures was published by Scott & Tanaka in 1986. Their geologic map of the western equatorial region of Mars presented a comprehensive view of tectonic structures pertaining to global scale mapping in the Tharsis region. Scott and Tanaka (1986) demonstrated the density of the tectonic structures proving, that compressional features occur mostly on the east part of Tharsis, while extensional features, mostly grabens, are concentrated close to Tharsis volcanoes (Knapmeyer et al., 2006). Those extensional features were suggested to be part of the global structural system, and evidence volcano-tectonic interactions (e.g. Banerdt et al., 1982; Mège & Masson, 1996). The main lines of the volcanic and tectonic evolution of the Tharsis province have been detailed in many works (e.g. Mège et al., 2003) and consequences for hydrology have been acknowledged (Phillips, 2001).

During the Noachian and Early Hesperian periods, Mars likely had significant snow and ice accumulation trapped in the Tharsis region (Cassanelli & Head, 2019). Glaciation-deglaciation cycles were interpreted to be involved in the formation of Hesperian valley networks such as Kasei Valles and Mangala Valles, based on morphological features at the surface similar to those found in glacial environments on Earth (Chapman & Tanaka, 2002; Wilson & Head, 2004). Also, the morphology of more recent outflow channels has been explained by the occurrence of catastrophic floods of large volumes of abruptly released groundwater(e.g. Burr et al., 2009; Rodriguez et al., 2015). Some of the channels were incised in lava flows

CONTACT Anita Zambrowska azambrowska@cbk.waw.pl Centrum Badań Kosmicznych Polskiej Akademii Nauk (CBK PAN), Bartycka 18A, Warszawa 00-716, Poland

Supplemental map for this article can be accessed at https://doi.org/10.1080/17445647.2024.2419467

© 2024 The Author(s). Published by Informa UK Limited, trading as Taylor & Francis Group on behalf of Journal of Maps
This is an Open Access article distributed under the terms of the Creative Commons Attribution License (http://creativecommons.org/licenses/by/4.0/), which permits unrestricted use, distribution, and reproduction in any medium, provided the original work is properly cited. The terms on which this article has been published allow the posting of the Accepted Manuscript in a repository by the author(s) or with their consent.

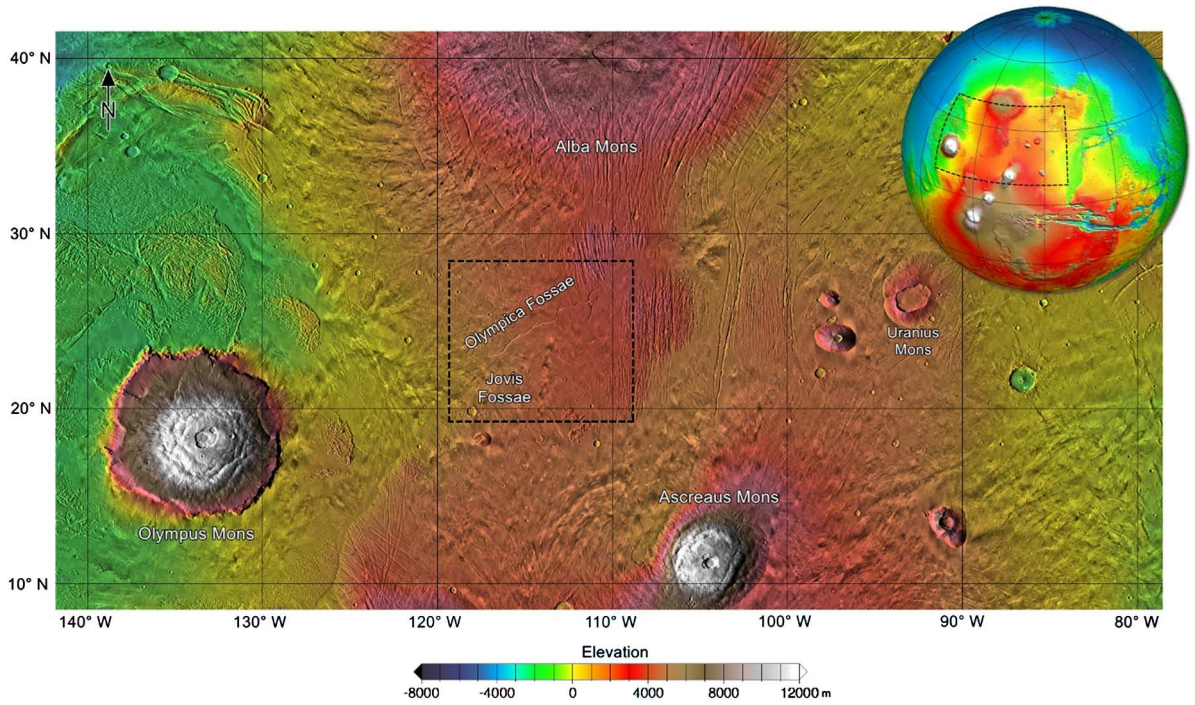

Figure 1. Topography of the Tharsis region with the location of Olympica Fossae and Jovis Fossae with an elevation bar. A polygon marks the area mapped in this study. Globe inset shows the displayed area on Mars. Image background: MOLA shaded relief by NASA/MGS/MOLA Science Team.

which may be only a few hundred million years old. The dissimilarities in the water cycle between Mars and Earth likely result from differences on both planets in the initial water budget, crustal evolution, and the consequences of lower gravity on volatile stability and atmospheric escape (Mangold et al., 2016).

The Olympica-Jovis Fossae hydrological system formed between the large volcanic edifices of northern Tharsis and Olympus Mons (Figure 1). The Olympica-Jovis Fossae system extends from Ceraunius Fossae, a network of grabens filled with lava, to Jovis Tholus, a collapsed caldera volcano. This system is part of the development of channels within the Amazonian deposits of the Tharsis volcanoes (Hargitai & Gulick, 2018; Sutton et al., 2022), and provides one of the best opportunities to understand the development of young channels on Mars. The earliest geologic map from the Tharsis region includes geologic units and a system of grabens (Scott & Tanaka, 1986). It was then updated, and marked the Olympica Fossae as an outflow channel (Tanaka et al., 2014). Vijayan and Sinha (2017) identified outflow channels in a channel system at the southwestern tip of Jovis Fossae, but their detailed local map does not encompass the entire Olympica – Jovis Fossae system. A more recent map of channels of the east of Olympus Mons includes the Olympica – Jovis Fossae as a part of this extended channelized region (Hargitai & Gulick, 2022). It does not identify individual channel units and cross-cutting relationships between them.

To provide a more holistic view of the region and mitigate limitations with previous mapping efforts, we present a detailed geologic map of the Olympica-Jovis Fossae hydrological system (Online Supplement). By morphologically classifying the mapped valleys and channels, and analyzing cross-cutting relationships, we can infer a minimum number of hydrological events.

2. Data, software, and methods

To map morphological and geological features, we used visible imagery from the Mars Reconnaissance Orbiter (MRO) Context Camera (CTX) with a resolution of 6 meters per pixel (Fergason et al., 2021; Malin et al., 2007) and MRO High-Resolution Imaging Science Experiment (HiRISE) camera with a resolution of 25 cm per pixel (McEwen et al., 2007). To constrain the intersecting relationships between channels we used the newest DEM topography data (2021–2023) from the Mars Express High Resolution Stereo Camera (HRSC) with a resolution of ~20–40 meters per pixel (Jaumann et al., 2007; Neukum et al., 2004), and from the ExoMars Trace Gas Orbiter, Colour and Stereo Surface Imaging System (CaSSIS) with a resolution of 4.8 meters per pixel (Thomas et al., 2017). The daytime infrared global mosaic from the Mars Odyssey Thermal Emission Imaging System (THEMIS) with a resolution of ~100 meters per pixel (Edwards et al., 2011), in combination with the CTX images, allowed us to identify

Table 1. Description of the mapped units and geological features along with their symbology and interpretation of possible origin.

Image of type area	Unit name	Description	Interpretation
	Main channel	Linear, narrow, troughs of width 200–600 m. In the central part mostly meandering channels. The tripple-junction and junction of Olympica and Jovis Fossae controlled by deep tectonic structures (grabens) with NS orientation.	A tectonic origin probably related to catastrophic outburst floods or/and volcanic processes.
	Anastomosing channel	A network of interconnected shallow (~20 m) channels with mid-channel bars. The length of the channels is up to 350 km.	Channel formation likely involves fluvial processes requiring the presence of large volumes of fluid, probably water.
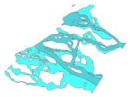	Outflow channel	Channels spanning 30 km in width and 40 km in length with streamlined islands indicating the direction of the flow. Channels associated with fissures/grabens, which are oriented along the SW-EW direction.	Fluvial outflow originating from nearby breaches of fissures/grabens.
	Meandering channel	Narrow (up to 400 m) meandering channels with parallel banks and no visible source of flow. Length up to 70 km.	Can be the result of fluvial or ultramafic lava flow erosion from a single source.
	Terraced valley	Consists of flat-topped platforms located along the Olympica Fossae. The surfaces of the platforms are flat and dipping at a low angle (~2°) toward 15–20° steep main channel walls. Width up to 7 km and depth up to 500 m.	Remnants of former floodplain surfaces that were incised by water flow.
	Glacial lineation	Linear depressions in the bedrock along the central and western part of Olympica Fossae. This pattern continues south-westward and ends ~10 km by the junction of Olympica and Jovis Fossae. Length and width of the lineated surface are up to 13–30 and 8 km, respectively.	Likely developed by an ice stream/glacier along the Olympica Fossae.

Image of type area	Unit name
Impact craters of diameter < 15 km	
	Rampart ejecta
	Simple ejecta
	Crater palimpsest
	Crater rim
Impact craters of diameter > 15 km	
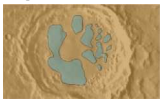	Infilling
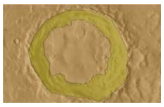	Faulted rim
	Crater floor

Image of type area	Unit name	Description	Interpretation
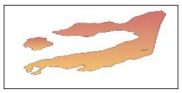	Amazonian lava flow from fissure	Lobate sheets of dense fluid extend for tens to hundreds of kilometers in length.	Lava originating from volcanic fissures.

(*Continued*)

Table 1. Continued.

Image of type area	Unit name	Description	Interpretation
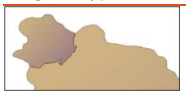	Late Hesperian lava flow	Widespread, covering over 800 km^2 sheet of rough surface texture material. Length of a few kilometers to hundreds of kilometers.	Voluminous lava flows erupted from several volcanoes in the Jovis Tholus region (18.40°N, 117.40°W).
	Lava channel	Channels with levees. Length up to hundreds of kilometers.	Lava flow originating from volcanic fissures and/or vents.
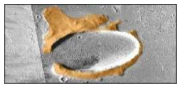	Volcanic construct/ crater	Elongated open rim filled surrounded by ejecta.	Breached volcanic edifice with eruptive crater, or impact crater from an oblique impact.
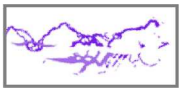	Lava tubes	Partly covered sinuous channels.	Lava tubes.
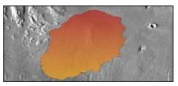	Volcanic edifice	Shield structure covered by lava flows.	Volcanic edifice.
	Volcanic vent/fissure	Circular or linear depression on top of lava flows. Extend from tens to hundreds of kilometers.	Volcanic vent, fissure.
	Amazonian airfall deposit	Smooth unit at HiRISE image scale forming a layer of thickness up to ~20 meters of layer on the walls of Olympica and Jovis Fossae.	Dust and/or pyroclastic deposits.
	Early Amazonian volcanic unit	Rugged and pitted terrain covering ~250,000 km^2 with lobate flows meters to tens of meters thick and hundreds of kilometers long.	Lava flows erupted from volcanoes and fissures around Ceraunius Fossae.
	Hesperian Unit	Narrow, parallel troughs. Several kilometers wide, 100–800 m deep.	Grabens.
	Hesperian highland edifice unit	Unit cover around 4 500 km^2. Rugged morphology.	Intensely eroded lava flow.
	Early Amazonian/Late Hesperian edifice unit	Rugged lobate flows. Surface area covered: ~20,000 km^2	Eroded lava flows from an unknown source.

and map the outlines of lava flows. All imagery data were integrated into a geographic information system (GIS) in the open-source QGIS software (https://qgis.org/en/site/). The geologic map was produced with the Geographic Coordinate System Mars 2000 spheroid projection system with a central meridian at 180 degrees. The THEMIS basemap was used as the optical background, and the HRSC – derived Digital Elevation Model (DEM) was used to present the topography.

The map covers ~1.1*10^6 km^2 in the latitude and longitude ranges 19.50°N – 28.03°N and 109.15°W – 119.40°W. We mapped water and lava channels, lava flows, glacial landforms, fractures, and impact craters. We also determined chronological relationships between the channels, summarized in a chart of 28 mapped fluvial channels and their stratigraphic position with respect to the geological timescale for Mars (Werner & Tanaka, 2011). The defined ages of the Hesperian fractured terrain and Amazonian lava surfaces are based on Tanaka et al. (2014). The unit boundaries were refined by using higher-resolution mapping.

The boundaries of glacial and fluvial landforms, impact craters of diameter larger than 200 m, and landforms were primarily mapped on CTX imagery. The boundaries of individual lava flows were mapped using THEMIS data and verified with CTX imagery. We grouped the mapped channels based on morphological characteristics (Table 1) identified on CTX, CaSSIS, and HiRISE imagery. Some linear features in the CTX imagery data were interpreted as grabens, cracks, and normal faults. The airfall unit was interpreted and mapped using

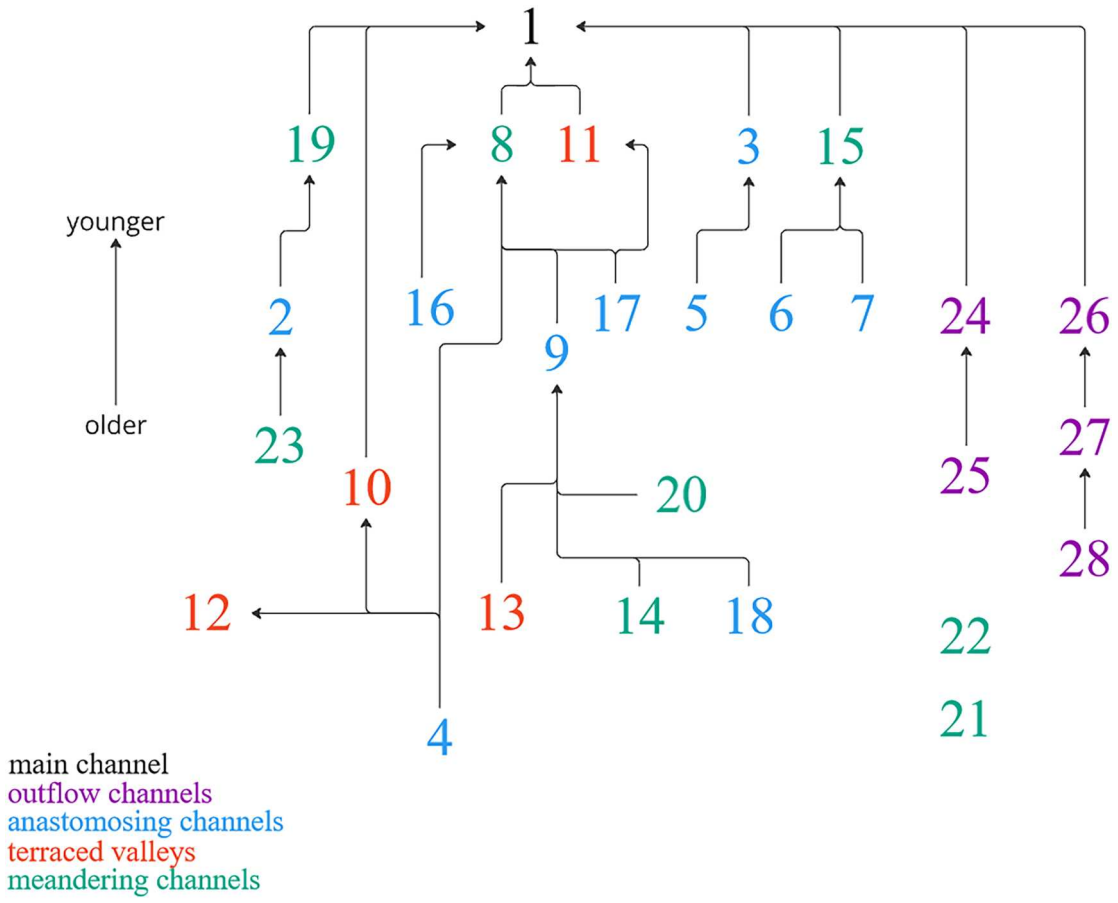

Figure 2. Chart of cross-section relationships between 28 mapped fluvial channels. Arrowheads indicate younger flows.

HiRISE images. The map also shows interpreted glacial lineations observed on CTX, CaSSIS, and HiRISE imagery, located in the central part of Olympica – Jovis Fossae. Arrows indicate water and lava flow direction.

3. Description of units

Table 1 provides a detailed description and interpretation of the mapped units. The map presents five major groups of geological and morphological units (see online Supplementary): geological structures defined as linear cracks, grabens, and three generations of faults; volcanic features which include volcanic vents, lava flows, lava channels, and the direction of lava flows; basement units, from oldest to youngest: Noachian/Hesperian highland edifice unit, Hesperian unit, Hesperian/Early Amazonian unit, the most extensive Early Amazonian volcanic unit; (a) twenty-eight fluvial units grouped into five morphological types of channels: anastomosing channels, terraced valleys, meandering channels, outflow channels, and the main channel; (b) glacial lineations; (c) impact craters; and (d) airfall deposit unit. A general investigation of the mapped units reveals the correlation between volcanic activity on Tharsis and Amazonian flooding events. The geological map displays many lava flows and volcanic edifices, partially covering the Tharsis volcanic plains, that formed after the Amazonian flooding events.

(a) The chronology of the 28 fluvial units is presented as a chart (Figure 2), in which the relative ages and relationships between channels were determined from cross-cutting relationships. For example, channels 5, 6, and 7 may correspond to a single event, as well as channels 10–11, and 14–18. Morphologic analysis and chronology made the categorization of five channel groups possible.
- The oldest among the fluvial units are terraced valleys that resulted from variations in water level in channels (Garde, 2006). Both valleys 10 and 11 contain visible step-like features along the banks. Channel 11 reaches up to 5 km wide and 6 km long. Channel 10 is wider, reaching up to 7 km. The length of the channel is 14 km long. All of the mapped terraced valleys are partially preserved.
- The second oldest channel group includes anastomosing channels, which are shallower and wider than other channels. Anastomosing channeling can result from, among other factors, flow rate variation, composition of riverbed material, rate and distribution of sediment transport, and the width, depth,

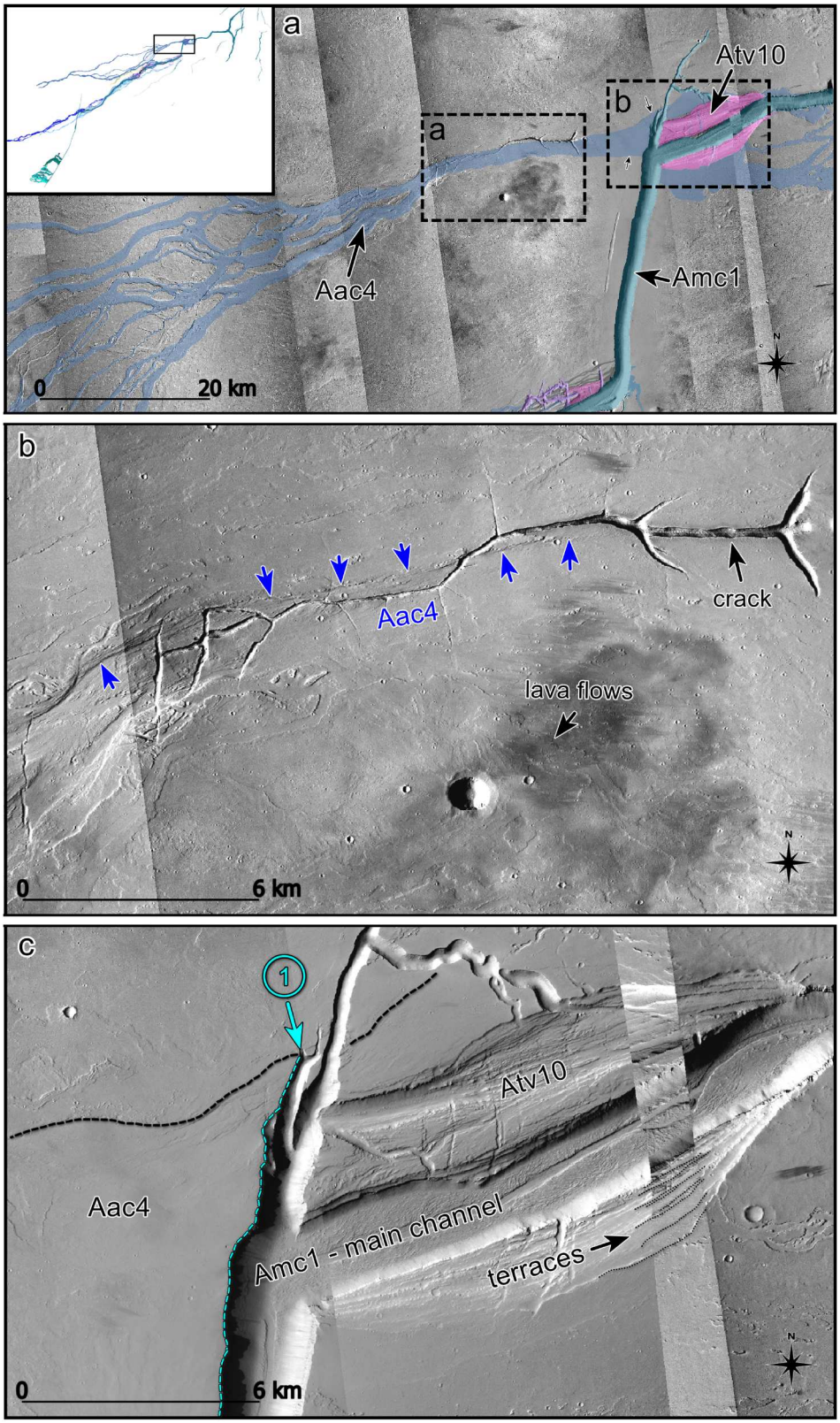

Figure 3. (a) Overview of the east part of Olympica Fossae with visible crack, anastomosing channel (blue), and terrace channel (pink); (b) crack as the possible origin of water outflow for the strongly eroded, anastomosing system shown in a; blue arrows indicate flow Abc4; (b) area of possible glacial regression/ice stream. Eroded channel floor of the terraced channel, with visible striations indicating flow orientation, terraces, and the main channel. ① cross-cutting boundary observed between channels Amc1 and Abc4. Image background: CTX scenes.

slope, and other morphometric bed properties (Ro Charlton, 2008). The floods on Tharsis could be released from surface fissures, as it is visible in channels 2, 3, and 5. The source of channel 4 is a branching crack system (Figure 3).

- Due to the absence of cross-cutting relationships with other channels, the relative age of

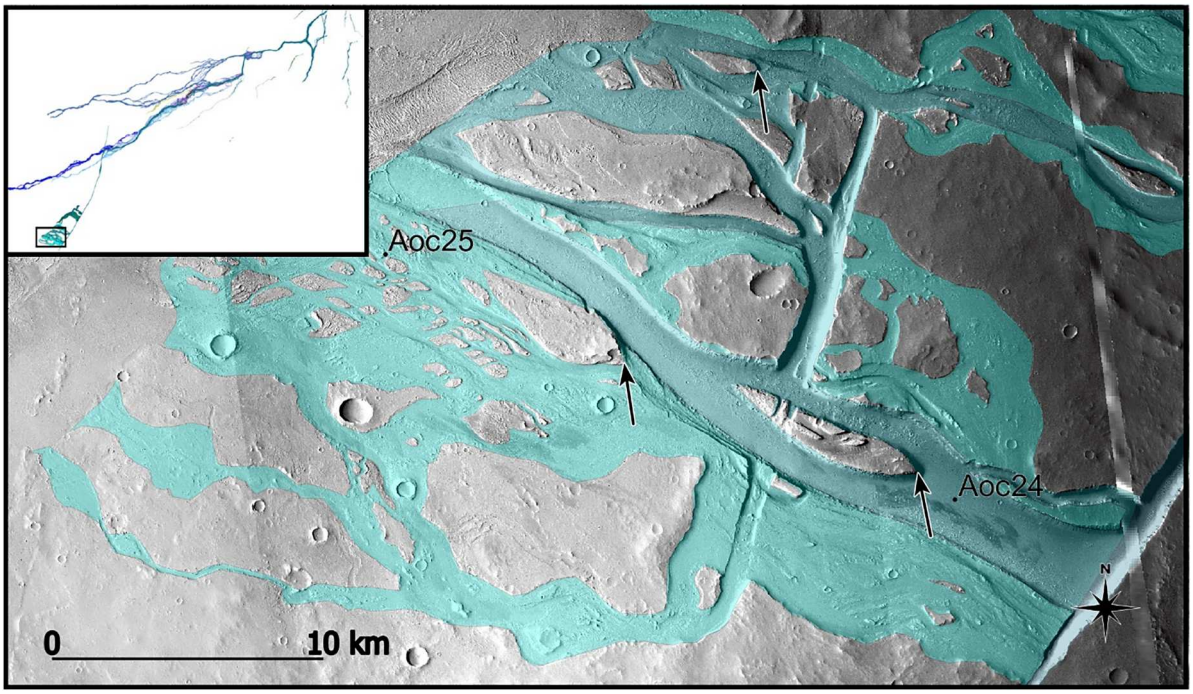

Figure 4. Example of outflow channels with streamlined islands indicating the direction of water flow. The black rectangle in the inset shows the location in the Olympica-Jovis system. The arrows point out the upstream tips of the streamlined islands. Image background: CTX imagery.

meandering channels is usually difficult to estimate. Geologic mapping reveals that channel 19 is the longest (135 km), with a width of ~ 250 m. The source of the flow of channel 19 is a fissure, but the upper course of channel 22 is coming from the Hesperian highland edifice unit.

- Outflow channels located on the southwest part of the Olympica – Jovis Fossae (20. 52° N, 118.54°W) (Figure 4) are characterized by broad channels and streamlined islands indicating the direction of the flow. The map shows that the outflows initiate from the Jovis Fossae fissure system. The collapse of the wall of the source fissure resulted in water flooding in the outflow channel 25. The walls of the fissures close to channels 26 and 27 are intact, which makes it difficult to determine where the water source was.
- The main channel represents the latest event and is the largest and most distinct feature in the mapped region. It heads at a network of elongated troughs (with NS tends) and cross-passing ridges (e.g. 25.40°N, 113.20°W or 22.50°N, 117.20°W). The depth of the main channel is different for each section of the channel, starting with ~900 m at the junction of troughs (26.06°N; 111.39°W) and decreasing to ~110 m at the junction between Olympica and Jovis Fossae (22.95°N, 117.14°W).

(b) Detailed mapping of Olympica Fossae channels reveals striated surfaces reminiscent of glacial lineations (Figure 7). They are located in the middle of the channel system (23.10°N, 116.61°W).

(c) The geologic map includes two types of craters, depending on diameter (Table 1). Impact craters < 15 km in diameter are either bowl-shaped (sometimes with a central peak), and display rampart or simple ejecta, palimpsest. The larger craters are flat-floored and show discontinuous infilling (Osinski & Pierazzzo, 2013).

(d) The airfall unit presented on the geologic map is a several meters thick layer of ash deposits or dust, visible on the walls of the junction of Olympica Fossae (26.00°N, 111.60°W). This layer is smooth at the HiRISE resolution scale. It is mostly concentrated near the source of Olympica Fossae. It may be composed of volcanic ash or dust. The TES Dust Cover Index (Ruff & Christensen, 2002) does not show dust thickness variations throughout the mapped area, suggesting that either this material is ash, or that the dust cover is thicker than what TES can reveal throughout the mapped area.

4. Discussion and conclusions

We presented a detailed geological map of the Olympica Fossae and Jovis Fossae region, which had never been studied in detail before. We identified 28 individual fluvial units, grouped into five

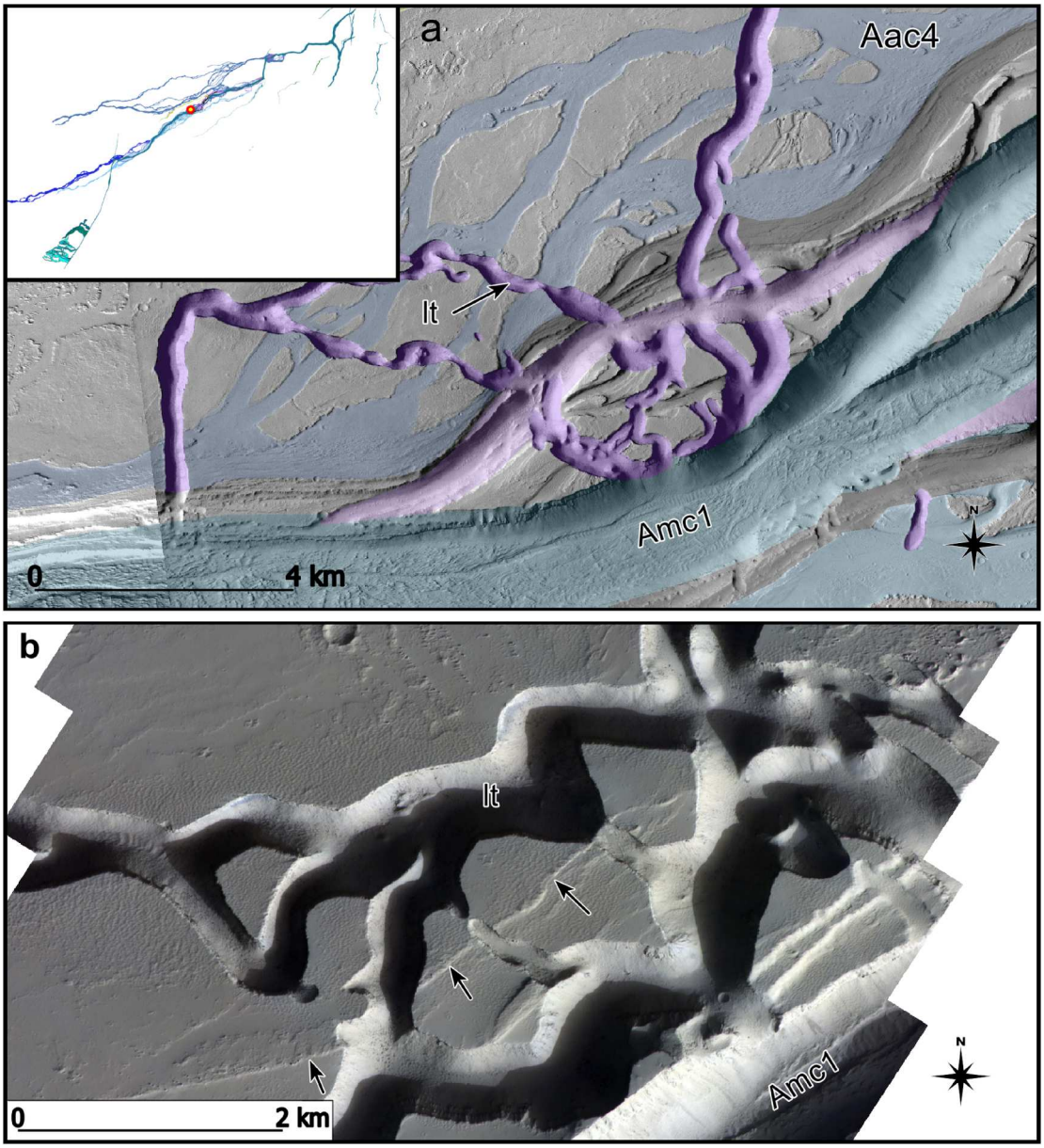

Figure 5. (a) Example of lava tubes (purple) in the middle part of Olympica Fossae. The red dot in the inset shows the location in the Olympica-Jovis system, CTX mosaic. (b) zoom of lava tubes (*lt)* with pit chains that cross-sected older channels, indicated by arrows on CaSSIS MY35_013159_026_0_NPB.

major types (outflow channels, meandering channels, anastomosing channels, the main channel, and terraced valleys) and a glacial unit in addition to impact craters, volcanic flows, volcanic edifices, vents, and tectonic structures. Volcanic units include long and narrow lava flows previously unmapped, and an abundance of small volcanic edifices that developed on the eastern side of the study area. Partly collapsed lava tubes that predate some of the water flows could be mapped in the central part of Olympica Fossae (Figure 5). The complex cross-cutting relationships between the channels are presented as a chart on the Main Map.

In Olympica and Jovis Fossae, morphological features such as terraces, longitudinal grooves, streamlined islands, and a network of anastomosing channels are interpreted as resulting from water flow. We did not find evidence of surface runoff. In contrast, some channels are observed to originate from fissures. This finding indicates that the water flowed from a groundwater reservoir. Consequently, magmatic heating is a plausible mechanism of water release. Whereas earlier mapping suggested (Tanaka et al., 2014) or is consistent with (Hargitai & Gulick, 2022) a single water flooding event, the presented map shows recurring water flows. Previous works on outflow channels usually advocated catastrophic floods from aquifers, possibly also related to igneous activity, in one or several flooding events (e.g. Burr et al., 2009; Carr, 2006). The originality of Olympica and Jovis Fossae in this respect is the absence of chaotic terrains upstream, which removes the main observable used to infer the catastrophic nature of the floods, as well as the very large number of channels, unreported at outflow

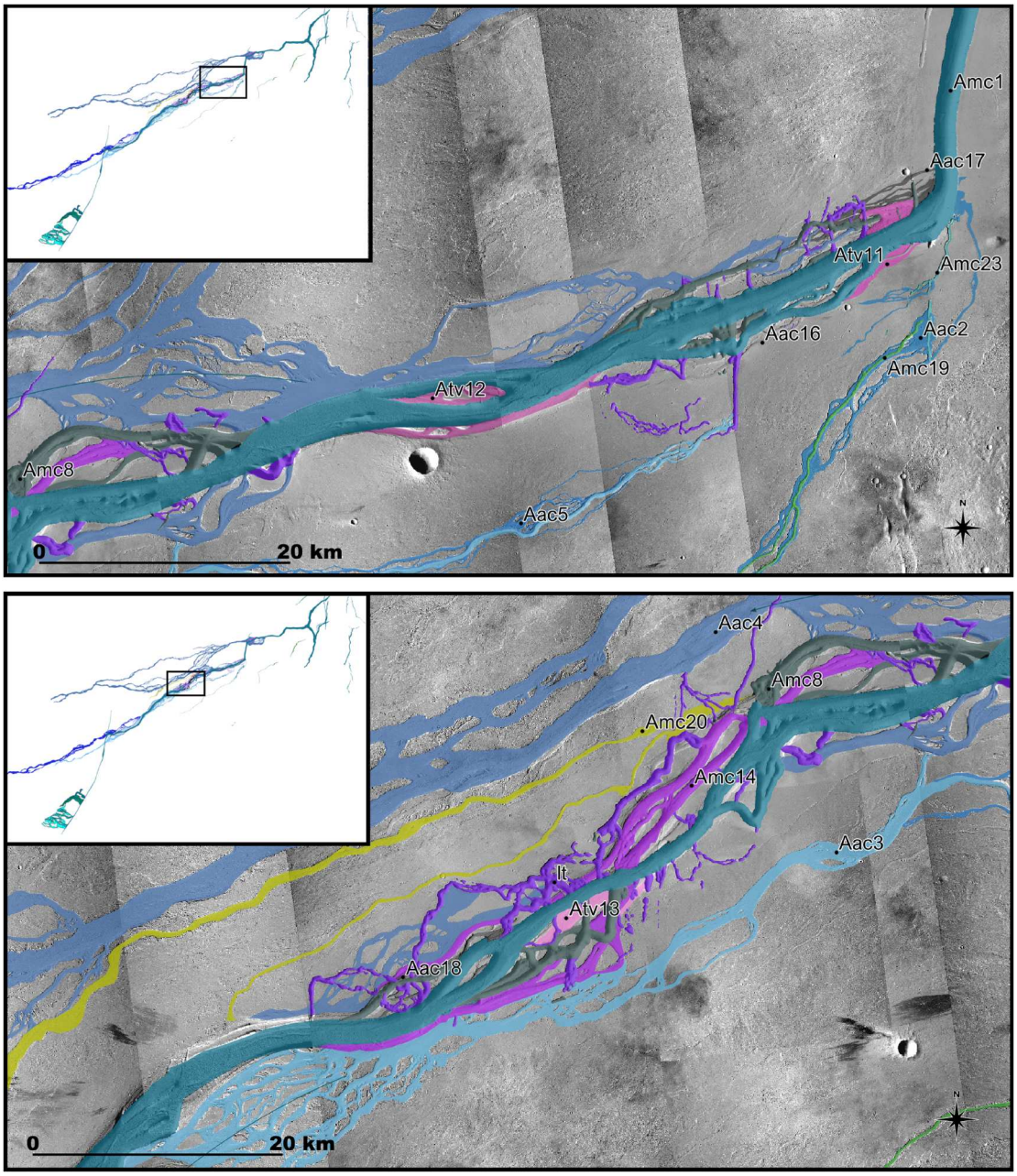

Figure 6. Complex generation of different types of channels are identified from their cross-cutting relationships; (a) east part of the Olympica – Jovis, (b) west part of the Olympica – Jovis. Insets show the location in the wider Olympica-Jovis system. For the color legend, please refer to Table 1 and the geological map in the Online supplementary material. Image background: CTX scenes.

channels of Hesperian or Amazonian age elsewhere so far. Some channels may have formed simultaneously, and cross-cutting relationships reported in the chronologic chart suggest a minimum of 5 distinct periods of flooding.

Outflow channels have alternatively been interpreted as the result of volcanic flows, supported by the observation of similar channel morphological properties on the Moon, Mercury, and Venus, where a volcanic origin appears to be required by the absence of crustal water (e.g. Leverington, 2011, 2021). In this interpretation, an ultramafic composition is probably required (Arndt et al., 2008; Huppert & Sparks, 1985; Staude et al., 2017). On Earth, ultramafic flows are of Precambrian age, a consequence of the required high source rock melting temperature. On Mars, ultramafic lava flows have been interpreted in ridged terrains in the Ladon basin, at similar Amazonian ages (Mège et al., 2023), consistent with a still active internal heating source (Durán et al., 2022) and suggesting that a volcanic origin of at least part of Olympica and Jovis Fossae flows cannot be ruled out. For instance, the bottom of the main channel, Amc1, displays a continuous lava flow. The map presented in this work, however, follows the dominant view for Hesperian and Amazonian channels on Mars that the channels are primarily formed in response to subsurface water release and water erosion, though interactions with igneous processes are likely (Huppert & Sparks, 1985).

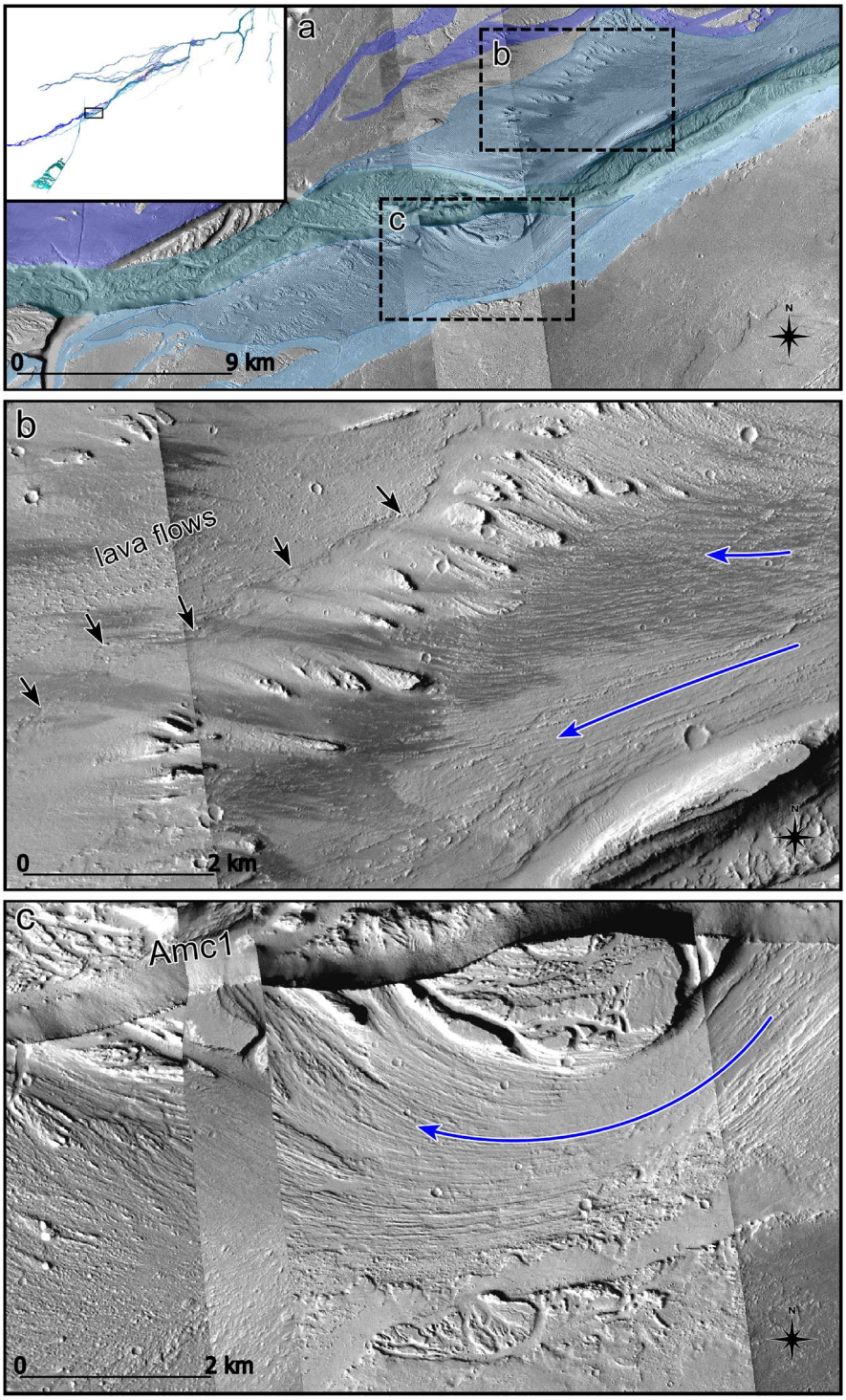

Figure 7. (a) Overview of lineations in the bedrock, probably formed by glacial flow along the channel. (b), (c) black arrows indicate the border of the earliest Amazonian lava flows. The blue arrow shows flow direction. The black rectangle in the inset shows the location in the Olympica-Jovis system. Image background: CTX scenes.

On high-resolution imagery, we observed lineations, which we interpret to be of glacial origin (Figure 7). This interpretation is based on similarities with lineations generated by fast flowing ice streams (Krabbendam et al., 2016) and is coherent with glacial landforms identified on the side volcanoes of the Tharsis dome and Olympus Mons (Head & Marchant, 2003; Head et al., 2005; Head & Weiss, 2014; Neukum et al., 2004; Parsons et al., 2020; Schiff & Gregg, 2022; Shean et al., 2007) formed during periods of high obliquity (Fastook et al., 2008; Forget et al., 2006).

The geologic map highlights the complexity of the Olympica and Jovis Fossae hydrologic system in space and time (Figure 6), providing a basis for understanding the recent hydrologic and volcanic activity at the top of the Tharsis dome. In particular, the diversity of channel dynamics implied by morphological observations testifies to a range of groundwater flow triggers

and surface flow conditions. The map also underlines the close association between volcanic activity and local control by the crustal fabric. These elements shall be taken into account in future efforts aiming at better understanding the igneous, tectonic, and hydrogeologic interactions in a region of Mars where igneous activity is probably still ongoing owing to the very recent age of the most recent lava flows identified (Hauber et al., 2011; Neukum et al., 2004; Pieterek et al., 2022; Richardson et al., 2017) and current seismicity, with InSight events located on both the eastern and western sides of the Tharsis dome (Drilleau et al., 2024).

Software

All collected data were stored in a digital georeferenced database and a digital geological map was designed using the 3.28 version of the free and open source QGIS software (QGIS.org, 2023, QGIS Geographic Information System, Open Source Geospatial Foundation Project, http://qgis.org).

Acknowledgements

We thank E. Hauber and S. Sutton for helpful discussions that improved this work.

Open data statement

CTX, HiRISE, and THEMIS data used in the process of mapping the study area were obtained through the National Aeronautics and Space Administration (NASA) Planetary Data System (http://pds.nasa.gov/) and the Mars Space Flight Facility of Arizona State University (http://www.mars.asu.edu/). The CaSSIS data were obtained from the repository for CaSSIS data (https://observations.cassis.unibe.ch/). Deutsches Zentrum für Luft – und Raumfahrt (DLR) provided the earliest data (2023), which covers the area of Jovis Fossae and the western part of Olympica Fossae.

CRediT author statement

Anita Zambrowska: Conceptualization, Methodology, Data curation, Investigation, Visualization, Writing – Original Draft, Daniel Mège: Conceptualization, Supervision, Validation, Writing – Review & Editing, Resources, Sam Poppe: Supervision, Validation, Writing – Review & Editing.

Disclosure statement

No potential conflict of interest was reported by the author(s).

Funding

This work is part of the doctoral studies of A. Zambrowska supported by the GeoPlanet Doctoral School and the Space Research Centre of the Polish Academy of Sciences. S. Poppe acknowledges support from the internal research fund of the Space Research Centre of the Polish Academy of Sciences.

References

Arndt, N., Lesher, M. C., & Barnes, S. J. (2008). *Komatiite*. Cambridge University Press. p.487 ⟨insu-00403305⟩.

Banerdt, W. B., Phillips, R. J., Sleep, N. H., & Saunders, R. S. (1982). Thick shell tectonics on one-plate planets: Applications to Mars. *Journal of Geophysical Research: Solid Earth*, *87*(B12), 9723–9733. https://doi.org/10.1029/JB087iB12p09723

Bouley, S., Baratoux, D., Matsuyama, I., Forget, F., Séjourné, A., Turbet, M., & Costard, F. (2016). Late Tharsis formation and implications for early Mars. *Nature*, *531* (7594), 344–347. https://doi.org/10.1038/nature17171

Burr, D. M., Wilson, L., & Bargery, A. S. (2009). Floods from fossae: A review of Amazonian-aged extensional–tectonic megaflood channels on Mars. *Megaflooding on Earth and Mars*, 194–208. https://doi.org/10.1017/CBO9780511635632.010

Carr, M. H. (2006). *The surface of Mars*. Cambridge University Press. 307 pp.

Carr, M. H., & Head, J. W. (2010). Geologic history of Mars. *Earth and Planetary Science Letters*, *294*(3-4), 185–203. https://doi.org/10.1016/j.epsl.2009.06.042

Cassanelli, J. P., & Head, J. W. (2019). Glaciovolcanism in the Tharsis volcanic province of Mars: Implications for regional geology and hydrology. *Planetary and Space Science*, *169*, 45–69. https://doi.org/10.1016/j.pss.2019.02.006

Chapman, M., & Tanaka, K. L. (2002). Related Magma–Ice interactions: Possible origins of Chasmata, Chaos, and surface materials in Xanthe, Margaritifer, and Meridiani Terrae, Mars. *Icarus*, *155*(2), 324–339. https://doi.org/10.1006/icar.2001.6735

Charlton, R. (2008). Chapter 8 – Channel form and behaviour. In *Fundamentals of fluvial geomorphology* (pp. 117–156). Routledge, Taylor & Francis Group.

Drilleau, M., Samuel, H., Garcia, R. F., Rivoldini, A., Perrin, C., Wieczorek, M., Lognonné, P., & Banerdt, W. B. (2024). Constraints on lateral variations of Martian crustal thickness from seismological and gravity field measurements. *Geophysical Research Letters*, *51*(4), e2023G–L105701. https://doi.org/10.1029/2023GL105701

Durán, C., Khan, A., Ceylan, S., Zenhäusern, G., Stähler, S., Clinton, J. F., & Giardini, D. (2022). Seismology on Mars: An analysis of direct, reflected, and converted seismic body waves with implications for interior structure. *Physics of the Earth and Planetary Interiors*, *325*, 106851. https://doi.org/10.1016/j.pepi.2022.106851

Edwards, C. S., Nowicki, K. J., Christensen, P. R., Hill, J., Gorelick, N., & Murray, K. (2011). Mosaicking of global planetary image datasets: 1. Techniques and data processing for thermal emission imaging system (THEMIS) multi-spectral data. *Journal of Geophysical Research*, *116* (E10008), 1–21. https://doi.org/10.1029/2010JE003755

Fastook, J. L., Head, J. W., Marchant, D. R., & Forget, F. (2008). Tropical mountain glaciers on Mars: Altitude-

dependence of ice accumulation, accumulation conditions, formation times, glacier dynamics, and implications for planetary spin-axis/orbital history. *Icarus*, *198*(2), 305–317. https://doi.org/10.1016/j.icarus.2008.08.008

Fergason, R. L., Hare, T. M., Mayer, D. P., Galuszka, D. M., Redding, B. L., Smith, E. D., Shinaman, J. R., Cheng, Y., & Otero, R. E. (2021). Mars 2020 terrain relative navigation flight product generation: Digital terrain model and orthorectified image mosaics. 51st Lunar and Planetary Science Conference. Abstract #2020. meetings/lpsc2020/pdf/2020.pdf.

Forget, F., Haberle, R. M., Montmessin, F., Levrard, B., & Head, J. W. (2006). Formation of glaciers on Mars by atmospheric precipitation at high obliquity. *Science*, *311*(5759), 368–371. https://doi.org/10.1126/science.1120335

Garde, R. J. (2006). River morphology, ISBN (13): 978-81-224-2841-4, New Age International (P).

Hargitai, H., & Gulick, V. (2018). Late Amazonian-aged channel and Island systems located east of Olympus Mons, Mars, Dynamic Mars. https://doi.org/10.1016/B978-0-12-813018-6.00004-2.

Hargitai, H., & Gulick, B. (2022). The channels east of Olympus Mons, Mars. *Journal of Maps*, *18*(2), 413–417. https://doi.org/10.1080/17445647.2022.2076622

Hauber, E., Brož, P., Jagert, F., Jodłowski, P., & Platz, T. (2011). Very recent and wide-spread basaltic volcanism on Mars. *Geophysical Research Letters*, *38*(10), L10201. https://doi.org/10.1029/2011gl047310

Head, J. W., & Marchant, D. R. (2003). Cold-based mountain glaciers on Mars: Western Arsia Mons. *Geology*, *31*, 641–644. doi:10.1130/0091-7613(2003)031<0641:CMGOMW>2.0.CO;2

Head, J. W., Neukum, G., Jaumann, R., Hiesinger, H., Hauber, E., Carr, M., Masson, P., Foing, B., Hoffmann, H., Kreslavsky, M., Werner, S., Milkovich, S., & van Gasselt, S. (2005). Tropical to mid-latitude snow and ice accumulation, flow and glaciation on Mars. *Nature*, *434*(7031), 346–351. https://doi.org/10.1038/nature03359

Head, J., & Weiss, D. (2014). Preservation of ancient ice at Pavonis and Arsia Mons: Tropical mountain glacier deposits on Mars. *Planetary and Space Science*, *103*, 331–338. https://doi.org/10.1016/j.pss.2014.09.004

Huppert, H. E., & Sparks, R. S. J. (1985). Komatiites I: Eruption and flow. *Journal of Petrology*, *26*(3), 694–725. https://doi.org/10.1093/petrology/26.3.694

Jaumann, R., Neukum, G., Behnke, T., Duxbury, T. C., Eichentopf, K., Flohrer, J., Gasselt, S. v., Giese, B., Gwinner, K., Hauber, E., Hoffmann, H., Hoffmeister, A., Köhler, U., Matz, K.-D., McCord, T. B., Mertens, V., Oberst, J., Pischel, R., Reiss, D., … Wählisch, M. (2007). The high-resolution stereo camera (HRSC) experiment on Mars express: Instrument aspects and experiment conduct from interplanetary cruise through the nominal mission. *Planetary and Space Science*, *55*(7), 928–952. https://doi.org/10.1016/j.pss.2006.12.003

Knapmeyer, M., Oberst, J., Hauber, E., Wählisch, M., Deuchler, C., & Wagner, R. (2006). Working models for spatial distribution and level of Mars' seismicity. *Journal of Geophysical Research: Planets*, *111*, E11006. https://doi.org/10.1029/2006je002708

Krabbendam, M., Eyles, N., Putkinen, N., Bradwell, T., & Arbelaez-Moreno, L. (2016). Streamlined hard beds formed by Palaeo-ice streams: A review. *Sedimentary Geology*, *338*, 24–50. https://doi.org/10.1016/j.sedgeo.2015.12.007

Leverington, D. W. (2011). A volcanic origin for the outflow channels of Mars: Key evidence and major implications. *Geomorphology*, *132*(3-4), 51–75. https://doi.org/10.1016/j.geomorph.2011.05.022

Leverington, D. W. (2021). Dry megafloods on Mars: Formation of the outflow channels by voluminous effusions of low viscosity lava. Chapter 4. In R. J. Soare, S. J. Conway, J.-P. Williams, & D. Z. Oehler (Eds.), *Mars geological enigmas* (pp. 61–93). Elsevier.

Malin, M. C., Bell, J. F., Cantor, B. A., Caplinger, M. A., Calvin, W. M., Clancy, R. T., Edgett, K. S., Edwards, L., Haberle, R. M., James, P. B., Lee, S. W., Ravine, M. A., Thomas, P. C., & Wolff, M. J. (2007). Context camera investigation on board the Mars Reconnaissance Orbiter. *Journal of Geophysical Research*, *112*(E5), E05S04. https://doi.org/10.1029/2006JE002808

Mangold, N., Baratoux, D., Witasse, O., Encrenaz, T., & Sotin, C. (2016). Mars: A small terrestrial planet. *The Astronomy and Astrophysics Review*, *24*(1), 15. https://doi.org/10.1007/s00159-016-0099-5

McEwen, A. S., Eliason, E. M., Bergstrom, J. W., Bridges, N. T., Hansen, C. J., Delamere, W. A., Grant, J. A., Gulick, V. C., Herkenhoff, K. E., Keszthelyi, L., Kirk, R. L., Mellon, M. T., Squyres, S. W., Thomas, N., & Weitz, C. M. (2007). Mars reconnaissance orbiter's high resolution imaging science experiment (HiRISE). *Journal of Geophysical Research: Planets*, *112*(E5), E05S02. https://doi.org/10.1029/2005JE002605

Mège, D., Cook, A. C., Garel, E., Lagabrielle, Y., & Cormier, M. H. (2003). Volcanic rifting at Martian grabens. *Journal of Geophysical Research: Planets*, *108*(E5), 5044. https://doi.org/10.1029/2002JE001852

Mège, D., Gurgurewicz, J., Massironi, M., Pozzobon, R., Togonon, G., Pajola, M., Tornabene, L. L., Lucchetti, A., Baschetti, B., Davis, J. M., Hauber, E., De Toffoli, B., Doute, S., Keszthelyi, L., Marinangeli, L., Perry, J., Pommerol, A., Pompilio, L., Pio Rossi, A., … Thomas, N. (2023). Hydrothermal alteration of ultramafic rocks in Ladon Basin, Mars – insights from CaSSIS, HiRISE, CRISM, and CTX. *Journal of Geophysical Research: Planets*, *128*. https://doi.org/10.1029/2022JE007223

Mège, D., & Masson, P. (1996). A plume tectonics model for the Tharsis province, Mars. *Planetary and Space Science*, *44*(12), 1499–1546. https://doi.org/10.1016/S0032-0633(96)00113-4

Neukum, G., Jaumann, R., Hoffmann, H., Hauber, E., Head, J. W., Basilevsky, A. T., Ivanov, B. A., Werner, S. C., van Gasselt, S., Murray, J. B., & McCord, T. (2004). Recent and episodic volcanic and glacial activity on Mars revealed by the high resolution stereo camera. *Nature*, *432*(7020), 971–979. https://doi.org/10.1038/nature03231

Osinski, G. R., & Pierazzo, E. (2013). Chapter 1, Impact cratering: Processes and products. In G. R. Osinski & E. Pierazzo (Eds.), *Impact cratering* (pp. 1–20). Wiley-Blackwell.

Parsons, R. A., Kanzaki, T., Hemmi, R., & Miyamoto, H. (2020). Cold-based glaciation of Pavonis Mons, Mars: Evidence for moraine deposition during glacial advance. *Progress in Earth and Planetary Science*, *7*(1), 13. https://doi.org/10.1186/s40645-020-0323-9

Phillips, R. J. (2001). Ancient geodynamics and global-scale hydrology on Mars. *Science*, *291*(5513), 2587–2591. https://doi.org/10.1126/science.1058701

Pieterek, B., Ciazela, J., Lagain, A., & Ciazela, M. (2022). Late amazonian dike-fed distributed volcanism in the Tharsis volcanic province on Mars. *Icarus*, *386*, 115151. https://doi.org/10.1016/j.icarus.2022.115151

Richardson, J. A., Wilson, J. A., Connor, C. B., Bleacher, J. E., & Kiyosugi, K. (2017). Recurrence rate and magma effusion rate for the latest volcanism on Arsia Mons, Mars. *Earth and Planetary Science Letters*, *458*, 170–178. https://doi.org/10.1016/j.epsl.2016.10.040

Rodriguez, J. A. P., Platz, T., Gulick, V., Baker, V. R., Fairén, A. G., Kargel, J., Yan, J., Miyamoto, H., & Glines, N. (2015). Did the Martian outflow channels mostly form during the Amazonian period? *Icarus*, *257*, 387–395. https://doi.org/10.1016/j.icarus.2015.04.024

Ruff, S. W., & Christensen, P. R. (2002). Bright and dark regions on Mars: Particle size and mineralogical characteristics based on thermal emission spectrometer data. *Journal of Geophysical Research: Planets*, *107*(E12), 2–1–2–22. https://doi.org/10.1029/2001je001580

Schiff, N. L. G., & Gregg, T. K. P. (2022). Probable ice-rich deposits on north-facing slopes in Alba Patera, Mars. *Icarus*, *383*, 115063. ISSN 0019-1035. https://doi.org/10.1016/j.icarus.2022.115063

Scott, D. H., & Tanaka, K. L. (1986). Geologic map of the western equatorial region of Mars. U.S. Geological Survey. https://doi.org/10.3133/i1802A

Shean, D. E., Head, J. W., Fastook, J. L., & Marchant, D. R. (2007). Recent glaciation at high elevations on Arsia Mons, Mars: Implications for the formation and evolution of large tropical mountain glaciers. *Journal of Geophysical Research: Planets*, *112*(E3), E03004. https://doi.org/10.1029/2006je002761

Staude, S., Barnes, S. J., & Le Vaillant, M. (2017). Thermomechanical erosion of ore-hosting embayments beneath komatiite lava channels: Textural evidence from Kambalda, Western Australia. *Ore Geology Reviews*, *90*, 446–464. https://doi.org/10.1016/j.oregeorev.2017.05.001

Sutton, S., Hamilton, C., Cataldo, V., Williams, D., & Bleacher, J. (2022). Sinuous channels east of Olympus Mons, Mars: Implications for volcanic, hydrological, and tectonic processes. *Icarus*, *374*, 114798. https://doi.org/10.1016/j.icarus.2021.114798

Tanaka, K. L., Skinner, J. A., Jr., Dohm, J. M., Irwin, R. P., III, Kolb, E. J., Fortezzo, C. M., Platz, T., Michael, G. G., & Hare, T. M. (2014). Geologic map of Mars: U.S. Geological Survey Scientific Investigations Map 3292, scale 1:20,000,000, pamphlet 43 p. doi:10.3133/sim3292

Thomas, N., Cremonese, G., Ziethe, R., Gerber, M., Brändli, M., Bruno, G., Erismann, M., Gambicorti, L., Gerber, T., Ghose, K., Gruber, M., Gubler, P., Mischler, H., Jost, J., Piazza, D., Pommerol, A., Rieder, M., Roloff, V., Servonet, A., … Wray, J. J. (2017). The colour and stereo surface imaging system (CaSSIS) for the ExoMars trace gas orbiter. *Space Science Reviews*, *212*(3-4), 1897–1944. https://doi.org/10.1007/s11214-017-0421-1

Vijayan, S., & Sinha, Rishitosh K. (2017). Amazonian fluvial outflow channels in Jovis Tholus region, Mars. *Journal of Geophysical Research: Planets*, *122*(5), 927–949. http://dx.doi.org/10.1002/jgre.v122.5.

Werner, S. C. (2009). The global Martian volcanic evolutionary history. *Icarus*, *201*(1), 44–68. https://doi.org/10.1016/j.icarus.2008.12.019

Werner, S. C., & Tanaka, K. L. (2011). Redefinition of the crater-density and absolute-age boundaries for the chronostratigraphic system of Mars. *Icarus*, *215*(2), 603–607. https://doi.org/10.1016/j.icarus.2011.07.024

Wilson, L., & Head, J. W. (2004). Evidence for a massive phreatomagmatic eruption in the initial stages of formation of the Mangala Valles outflow channel, Mars. *Geophysical Research Letters*, *31*(15), L15701. https://doi.org/10.1029/2004GL020322

Geology of the Olympica Fossae and Jovis Fossae hydrologic system, Mars

Zambrowska, A., Mège, D., Poppe, S
Space Research Center Polish Academy of Science, Bartycka 18A, Warsaw, Poland

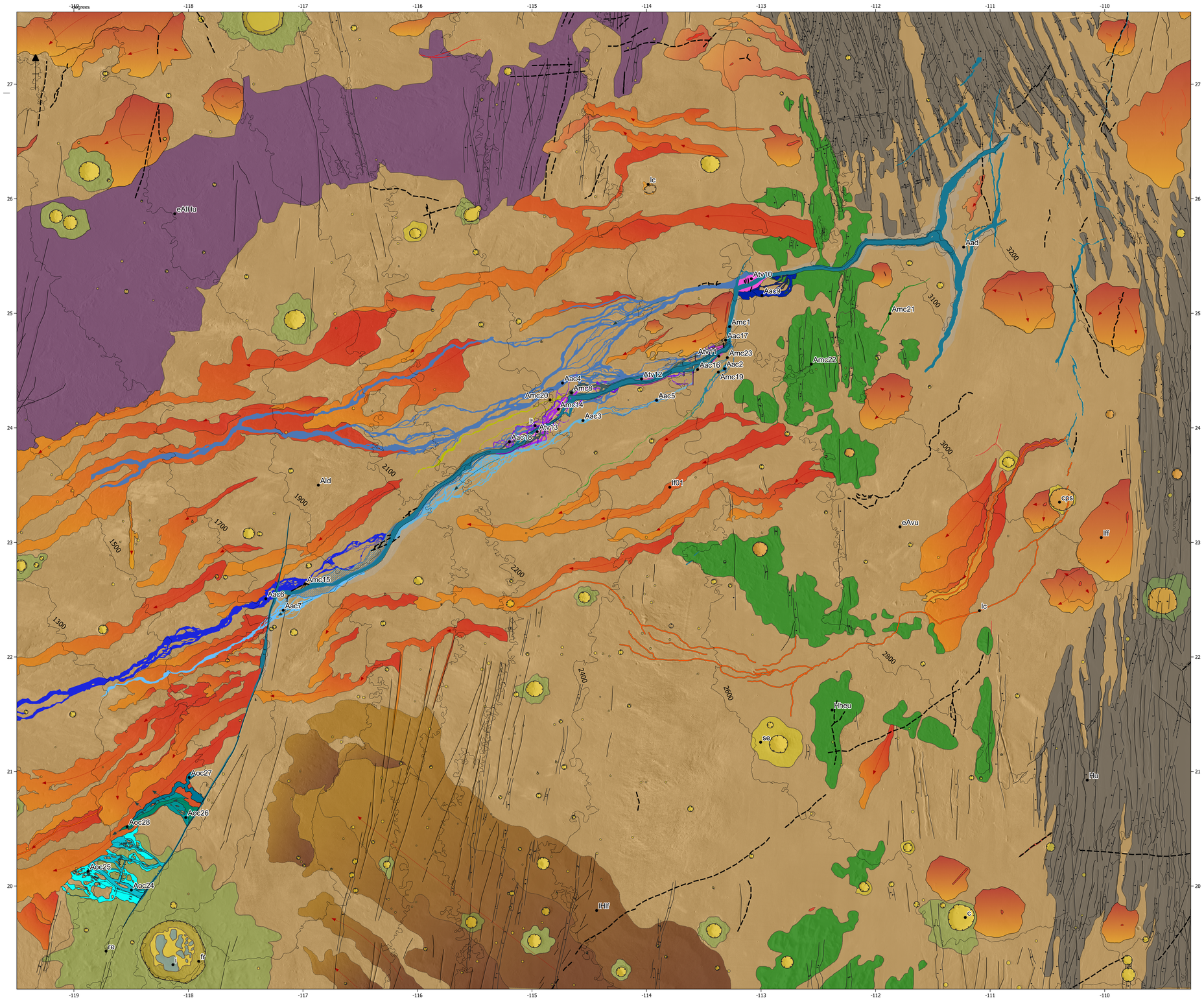

Scale at 0° latitude, Equirectangular Projection

Maping scale: 1:100000

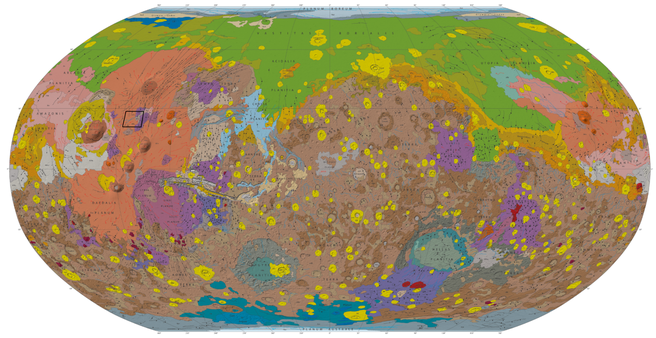

Legend:

Contact Types
- certain
- approximate

Geological Structures
- normal fault
- second generation of normal fault
- third generation of normal fault
- graben
- linear cracks

Glacial Lineations
- Agl - Amazonian glacial lineation

Fluvial Units
- Amc1 - main channel 1
- Aac2 - anastomosing channel 2
- Aac3 - anastomosing channel 3
- Aac4 - anastomosing channel 4
- Aac5 - anastomosing channel 5
- Aac6 - anastomosing channel 6
- Aac7 - anastomosing channel 7
- Amc8 - meandering channel 8
- Aac9 - anastomosing channel 9
- Atv10 - terraced valley 10
- Atv11 - terraced valley 11
- Atv12 - terraced valley 12
- Atv13 - terraced valley 13
- Amc14 - meandering channel 14
- Amc15 - meandering channel 15
- Aac16 - anastomosing channel 16
- Aac17 - anastomosing channel 17
- Aac18 - anastomosing channel 18
- Amc19 - meandering channel 19
- Amc20 - meandering channel 20
- Amc21 - meandering channel 21
- Amc22 - meandering channel 22
- Amc23 - meandering channel 23
- Aoc24 - outflow channel 24
- Aoc25 - outflow channel 25
- Aoc26 - outflow channel 26
- Aoc27 - outflow channel 27
- Aoc28 - outflow channel 28
- direction of water flow

Impact Craters
- re - rampart ejecta
- cf - crater floor
- se - simple ejecta
- cps - crater palimpsest
- i - infilling
- fr - faulted rim
- crater rim, d>1.5 km

Volcanic Units
- Alff - Amazonian lava flow from fissure
- lHlf - late Hesperian lava flow
- lt - lava tubes
- lava channel
- vc - volcanic construct
- direction of lava flow

Volcanic Edifices and Vents
- volcanic vent
- volcanic edifice
- volcanic fissure

Basement Units
- Aad - Amazonian airfall deposit
- Hu - Hesperian unit
- Hheu - Hesperian highland edifice unit
- eAlHeu - early Amazonian/late Hesperian edifice unit
- eAvu - early Amazonian volcanic unit

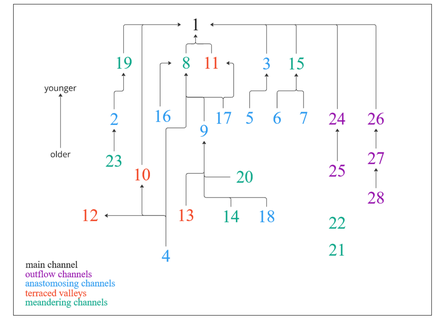

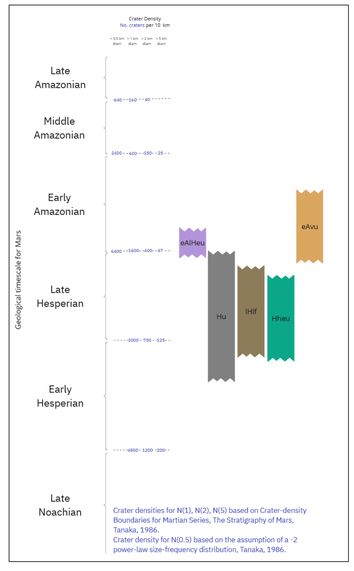

Used datasets:

Malin, M., MRO Context Camera Experiment Data Record Level 0 V1.0, MRO-M-CTX-2-EDR-L0-V1.0, NASA Planetary Data System, 2007
https://doi.org/10.17189/1520266

McEwen, A., Mars Reconnaissance Orbiter High Resolution Imaging Science Experiment, Experiment Data Record, MRO-M-HIRISE-2-EDR-V1.0, NASA Planetary Data System, 2007
https://doi.org/10.17189/1520179

Christensen, P.R., ODYSSEY THEMIS IR PBT V2.0, ODY-M-THM-5-IRPBT-V2.0, Mars Odyssey THEMIS Projected Products, NASA Planetary Data Systems, 2002
https://doi.org/10.17189/1520354

Smith, D.E., M.T. Zuber, G.A. Neumann, E.A. Guinness, and S. Slavney, Mars Global Surveyor Laser Altimeter Mission Experiment Gridded Data Record, MGS-M-MOLA-5-MEGDR-L3-V1.0, NASA Planetary Data System, 2003
https://doi.org/10.17189/1519460

Fergason, R. L, Hare, T. M., & Laura, J. (2018). HRSC and MOLA Blended Digital Elevation Model at 200m v2. Astrogeology PDS Annex, U.S. Geological Survey.
http://bit.ly/HRSC_MOLA_Blend_v0